Accelerator Development Department
BROOKHAVEN NATIONAL LABORATORY
Associated Universities, Inc.
Upton, New York 11973

AD/RHIC-43

RHIC TECHNICAL NOTE NO. 43

RHIC Internal Beam Dump
Preliminary Conceptual Design

A. J. Stevens

September 15, 1988

RHIC INTERNAL BEAM DUMP; PRELIMINARY CONCEPTUAL DESIGN

A. J. Stevens

I. Introduction

This note presents calculations relevant to the internal beam dump planned for RHIC. The dump location is assumed to be immediately downstream of Q4 on the inner arc, which is favorable as concerns both kicking the beam onto the dump face and quenching magnets downstream of the dump. The detailed considerations which led to this choice of locations are described elsewhere.[1]

An internal dump imposes severe requirements on the dump material due to the small size of the beam. As will be shown below, the dump could not withstand disposal of the design intensity at the maximum energy with its "natural" size. For this reason, a "sweeping" magnet is required to spread the beam on the dump face. In order to define criteria for both this magnet and the ejection kicker, two problems must be addressed: (1) conditions which will insure the integrity of the dump itself, and (2) conditions which minimize the likelihood of quenching downstream magnets. This note addresses these two areas of concern.

II. Materials/Survival Criteria

A. Dump Window

Heavy ion beams present a problem not encountered in high energy proton accelerators—high energy deposition density at the entrance face of the dump due to the Z^2 factor multiplying energy loss by ionization. Although, as mentioned above, a sweeping magnet will spread out the beam on the dump face, no sweeping can be accomplished during the 9 nsec. bunch-length time, so the first requirement of the dump is that the dump "window" be able to withstand the ionization energy loss of a single bunch.

As candidates for window materials (which must be exposed to the ring vacuum), we have considered alloys of titanium and steel. Although beryllium is theoretically superior to both these choices, it is an extremely hazardous (toxic) material. In order to avoid the special safeguards and working conditions which would be necessary if beryllium were used, we have (tentatively) excluded it as a possibility. Steel comes in a bewildering variety of "final products" which depend on both composition and processing conditions. The calculations made in this note are intended to be illustrative, rather than definitive, so we will take a non-"speciality" steel, AISI type 430, and Titanium alloy Ti-6A1-4V. The properties[2] of these materials are given in Table I.

The entrance energy density can be calculated in a straightforward manner given the machine parameters. From page 80 of the RHIC Conceptual Design,[3] the worst case ion in

Table I
Properties of Titanium and Steel at Room Temperature

	Melting Point (°C)	Specific Heat (cal/g°C)	Coefficient of Thermal Expansion ($\times 10^{-6}$/°C)	Elastic Modulus (Mpsi)	Tensile Strength (Kpsi)
Ti-6A1-4V	1649	0.135	9.54	16.5	170
AISI 430	1482	0.110	10.44	29	90

terms of the product of the number of ions per bunch times Z^2 is iodine. The 1-sigma beam size is given by:

$$X(Y) = (\beta_x(\beta_y) \cdot E/6)^{1/2}$$

where E is the unnormalized emittance containing 95% of the beam:

$$E = 10 \times 10^{-6}/(\beta\gamma) \quad \text{m-rad}$$

At top energy (and before intra-beam scattering increases the beam size) we obtain, for iodine immediately downstream of Q4,[4]

$$X(1\sigma) = 0.0418 \text{ cm}$$
$$Y(1\sigma) = 0.0644 \text{ cm}$$

The area of the beam ellipse on the dump face containing 39.3% of the beam is then

$$A_b = 0.00846$$

The energy density by ionization energy loss for an iodine bunch (containing 2.6×10^9 ions) is then

$$2.6 \times 10^9 \times (53)^2 \times .393 \times 1.5 \text{ MeV}/(\text{g/cm}^2) \times 3.82 \times 10^{-14} \text{ cal/MeV} \times (1/A_b)$$
$$= 19.44 \text{ cal/g}$$

We show the response of the materials considered here to this entrance deposition in Table II. In this table, we assume a room temperature of 20°C and calculate the thermal stress (static–in 1 dimension) from the formula of Sievers:[5] $s = \gamma \cdot Y \cdot \Delta T/2$ where γ is the coefficient of thermal expansion and Y is the elastic modulus given in Table I.

Although the titanium alloy is superior, specialty steels would reduce the margin of superiority shown in Table II. As mentioned above, this note is not intended to make a final

Table II
Entrance Material Response to Single Iodine Bunch

	Rise in Temp (°C)	Fraction of Melting Point (%)	Thermal Stress (Kpsi)	Stress/Tensile Strength (%)
Ti-6A1-4V	144	8.84	11.33	6.67
AISI 430	177	12.1	26.8	29.7

choice of materials, but to offer a "proof of principle". (Better Ti alloys are also available, e.g., Ti-6A1-6V-2Sn.)

What criteria should be adopted for the dump window is somewhat subjective. That a single dump should not exceed 10% of either the melting point or tensile strength would seem to be a reasonable choice, allowing for temperature dependence of material properties (heat capacity rises but tensile strength decreases with rising temperature) and possible fatigue effects. With this choice, the Ti alloy would seem to be satisfactory for a dump window.

The reader should note especially that the entire beam, 114[6] bunches, would destroy the window. (Beryllium would also melt.) If the sweeping magnet fails, destruction of the dump is an inevitable consequence. The number of ions per bunch is also limited to a value near that in the conceptual design. These constraints, dependence on the sweeper and a bunch intensity limitation, can only be relieved by extraction to an external dump.

B. Dump Interior

Having established that titanium is acceptable as a dump window, we now turn to the question of what should be behind the window. To address both this question and the problem of magnet quenching (next section), simulation of the hadronic cascade is required. We use a modified version of the FNAL program CASIM.[7,8]

As discussed in Ref. (8), whether the entrance deposition dominates the cascade build-up depends on the ion species in question, the transverse beam size, and the target material. For the limited purpose of the calculations presented in this section, we assume that the sweeper has blown up the beam area by a factor of 114 and has retained the relative X,Y size; specifically we consider a Gaussian beam with 1-sigma sizes of 0.45 cm (X) by 0.69 cm (Y). Fig. 1 shows the energy density per iodine ion within this beam size as a function of depth in a solid titanium block for iodine, gold, and protons. The curves have been normalized to the number of iodine ions (2.96×10^{11}) so that multiplication by this single number gives the actual energy density. Several interesting features are observed: (1) iodine is the worst case and its build-up peak is higher than its entrance deposition, reflecting the fact that iodine is also the worst case species in terms of the number of nucleons times the energy per nucleon, (2) for gold, the entrance density is closer to the build-up density (Z^2/A is highest for Au), and (3) protons dominate beyond a depth of

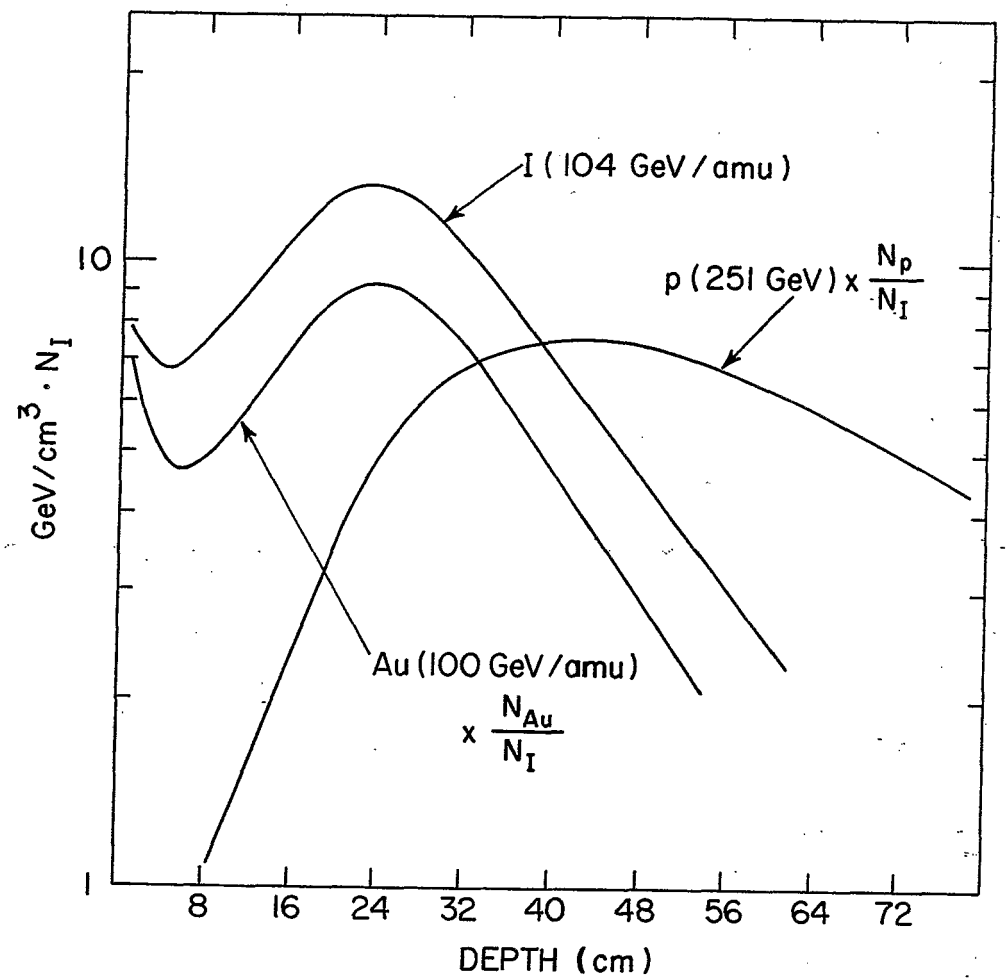

Fig. 1. Energy deposition density per iodine ion for R<0.4 cm vs. depth in a titanium cylinder. Transverse beam size is 0.45×0.69 cm^2 (see text).

~40 cm. (For both iodine and gold, the entrance deposition exceeds the build-up peak for beams with the small, unswept transverse size.)

The maximum deposition corresponds to a temperature rise in Ti of 248°C which is not within the criteria adopted above. Graphite (superior to all materials) must therefore be placed immediately behind the titanium window. Fig. 2 shows a sketch of a possible dump. The transition from graphite to steel is determined by the allowable temperature rise of the steel. The 1.2 meter distance shown in Fig. 2 allows the 10% of melting point criteria for a full (1.14×10^{13}) proton dump with the assumed beam size on a graphite/steel cylinder (i.e., a "dump" similar to that shown in Fig. 2 but without the hole in the middle). Such a cylinder with outer dimensions the same as those in Fig. 2 (R=40 cm, Z=2.8 m) would have energy leakages of 1.2% radially and 1.9% longitudinally for protons.

The actual leakage is dominated by energy emerging in the vacuum pipe "hole" and is a strong function of the radial depth at which the particles enter the dump face. This is shown in Fig. 3 as a function of the vertical coordinate (measured from the dump edge) for a parallel beam of protons whose X distribution is Gaussian with 1-sigma of 0.45 cm. The

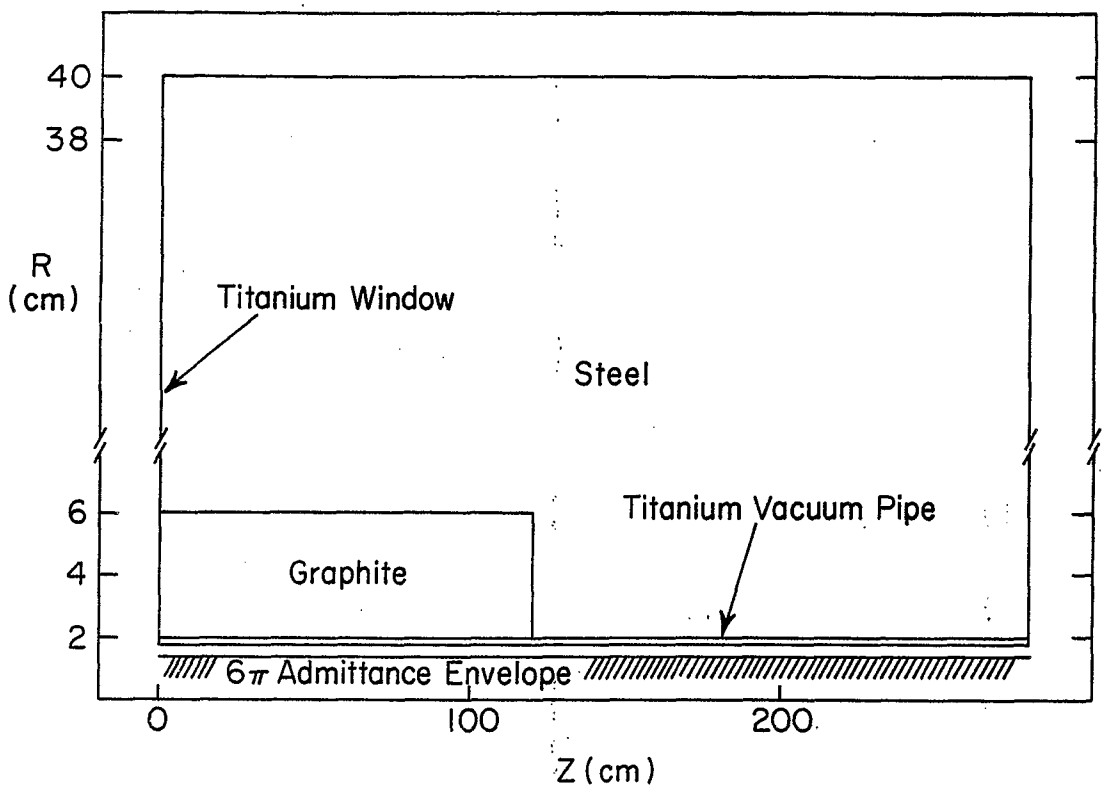

Fig. 2. Schematic sketch of beam dump.

circles in this figure show the total leakage and the triangles show the end leakage at small (R<2 cm) radius. It is only this small radius leakage which has a chance of quenching downstream magnets. As the distance from the dump edge approaches zero, the energy leakage becomes very high[8] and trajectories which scatter out of the edge with an infinitesimal change in direction become indistinguishable from those which barely miss the dump edge; both groups interacting elsewhere in the lattice. Empty R.F. buckets synchronized to the dump kicker rise time are planned to avoid this problem.[1]

Also shown in Fig. 2 is the 6π admittance envelope discussed in Ref. 1. The 3 mm gap between this envelope and the edge of the dump at Z=0 should probably not exist, but again, the results given here are not meant to be final. It should also be noted that the admittance envelope depends on the design value of the crossing point β.

III. Magnet Quenching

A schematic representation of the lattice downstream of the dump is shown in Fig. 4. Calculations were done only for 250 GeV/c incident protons which represent the worst case (maximum escaped energy) for the downstream magnets. In order to save computer time, a "biased" version of CASIM was used: specifically, only secondaries with energy greater than one third of the incident energy were propagated from first-generation interactions in the dump.[10]

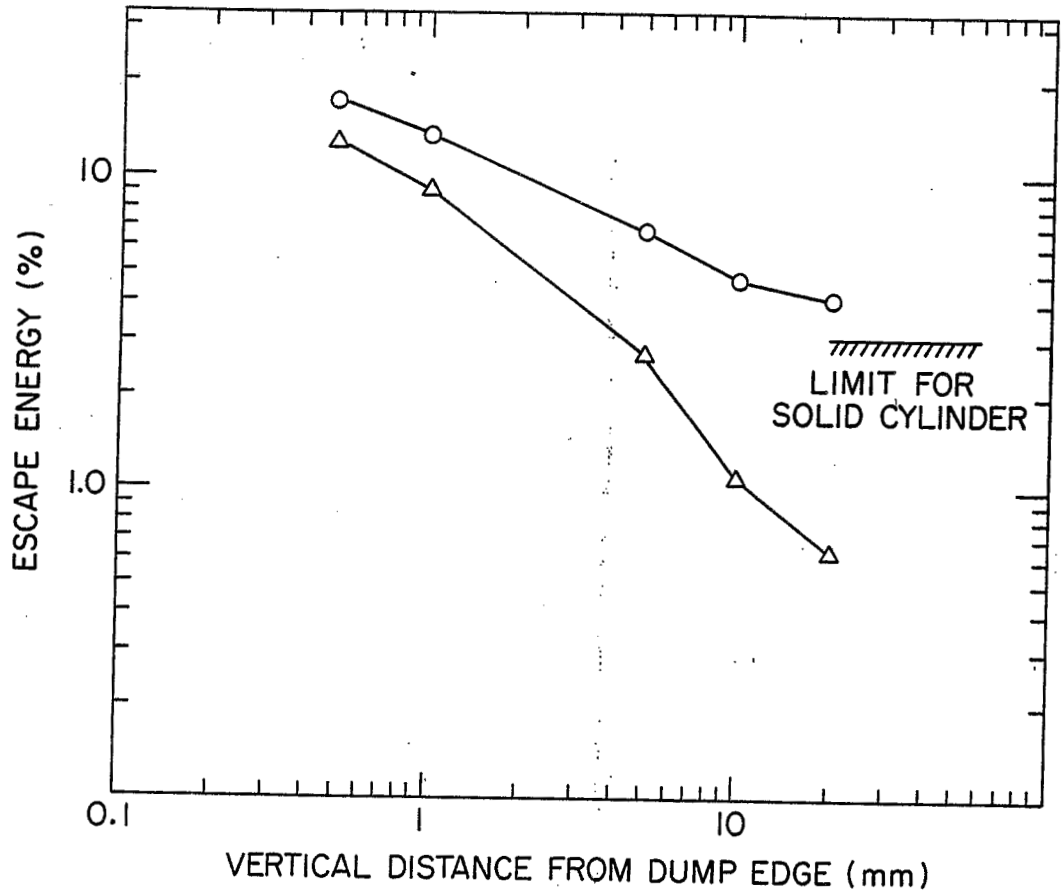

Fig. 3. Escaped energy vs. distance from dump edge. O for total escape. Δ for end escape with R<2 cm.

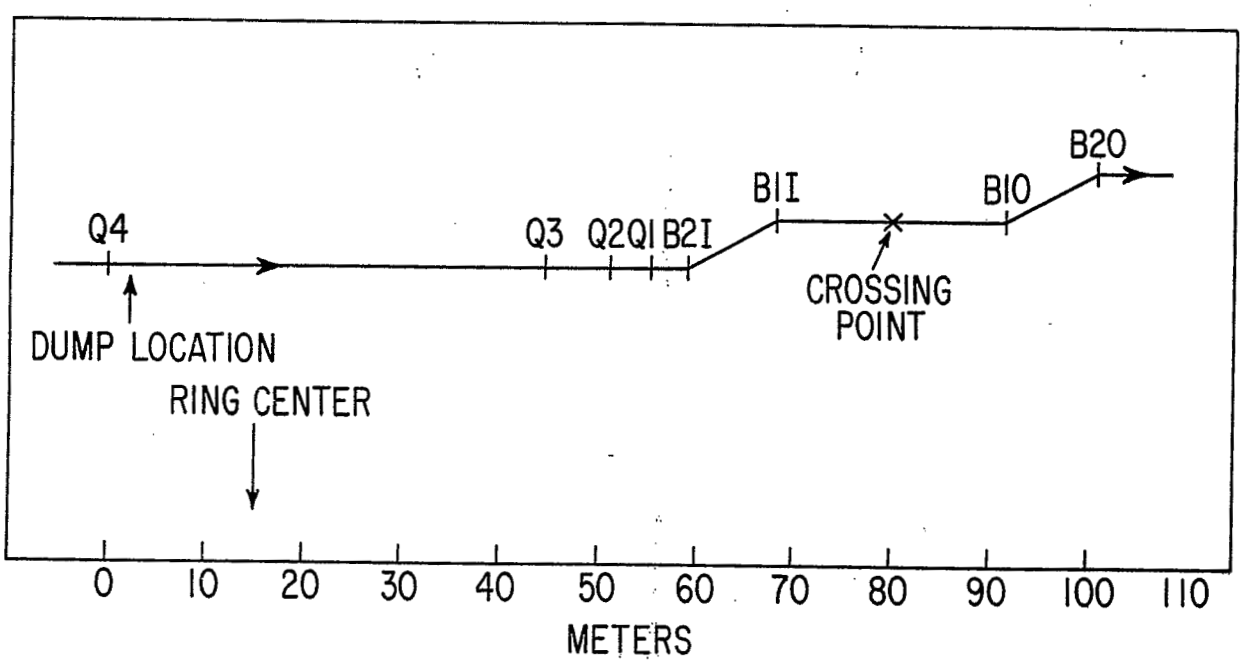

Fig. 4. Schematic representation of intersection region downstream of dump.

The magnetic fields were taken into account within the coil aperture which was taken as 4 cm (radius) in magnets Q3, Q2, Q1, B2I, and B2O and 5 cm in magnets B1I and B1O.[11] Energy deposition was calculated in the coil regions of these magnets as a function of length, radial depth, and azimuth.[12]

As discussed in the preceding section, energy escaping the dump is a strong function of the radial depth at which primaries enter the dump face. Figure 5 shows the energy deposition density averaged over the entire coil regions for protons incident at 1 mm depth (vertically) from the edge of the dump. The statistical errors shown are 1-sigma values

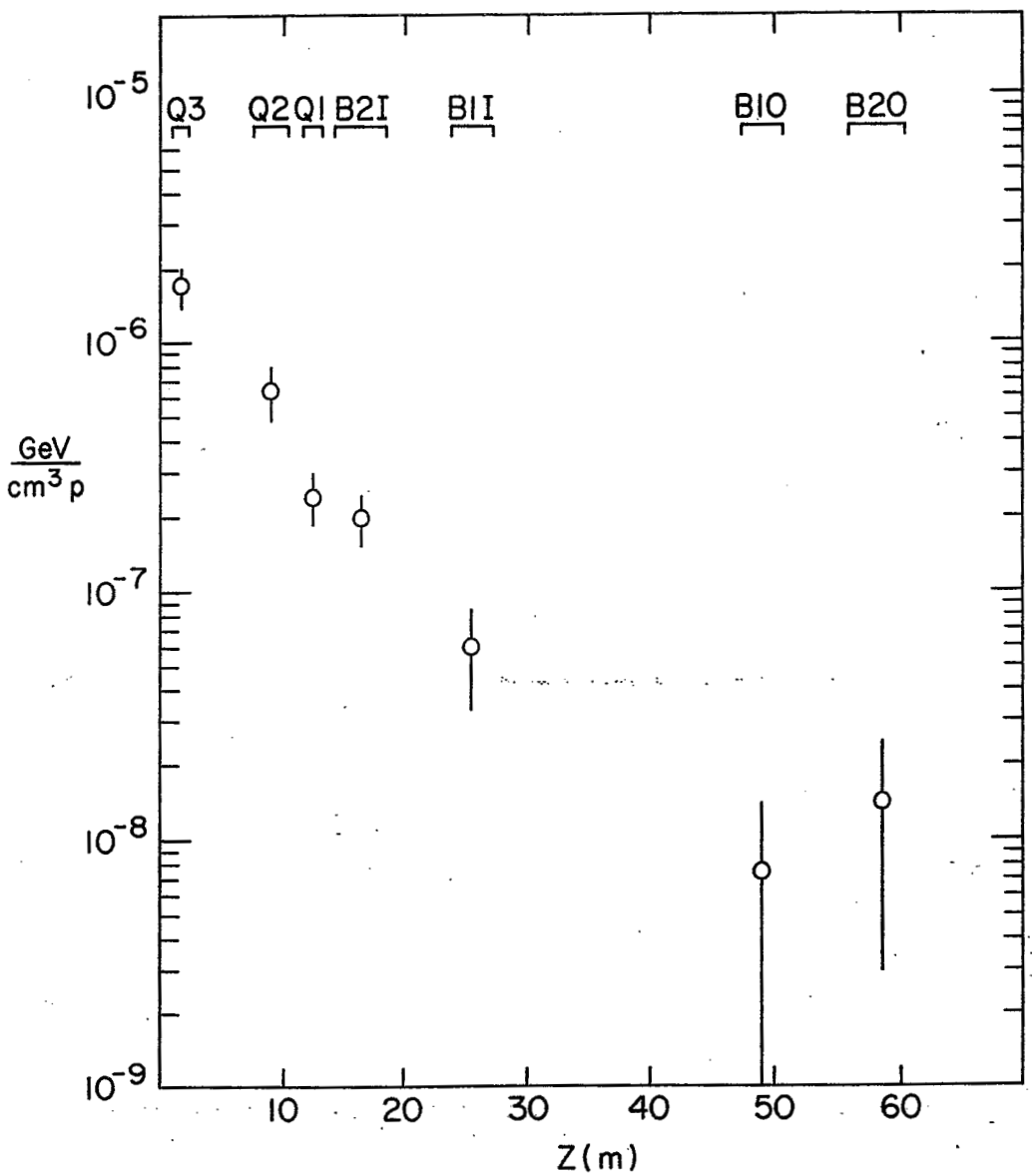

Fig. 5. Energy deposition density averaged over coils. Incident protons 250 GeV/c at 1 mm from edge of dump.

estimated from multiple runs but are not considered reliable at levels below ~10^{-8} GeV/cc per proton. At this depth for incidents, the CASIM results were examined for r, Z, and φ (magnet azimuth) dependence within each coil region. No statistically significant radial dependence was observed. The most dramatic Z dependence occurs in the B2I, B1I region as shown in Fig. 6. "Forward neutrals" emerging from the dump intercept the lattice between these two magnets and are believed responsible for this enhancement. Fig. 7 shows the φ dependence in the last Z bin in B2I. The enhancement on the "outboard" side of the magnet is consistent with a contribution from forward neutrals.

No contribution from first generation fast forward protons was clearly identified. This radiation had been calculated to be a dominant source of energy deposition in Isabelle

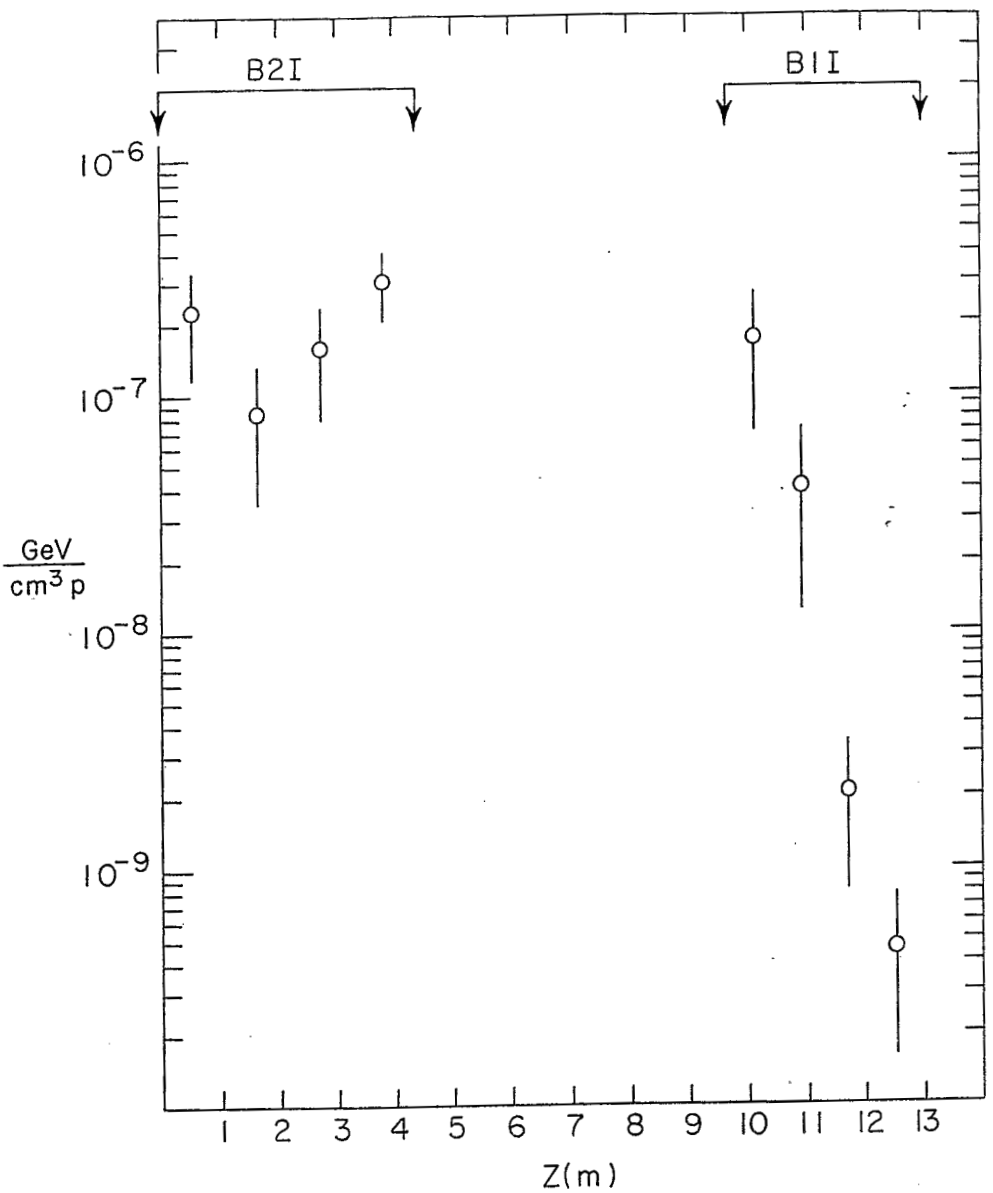

Fig. 6. Energy deposition averaged over r and φ as function of Z. Incident 250 GeV/c protons at 1 mm from edge of dump.

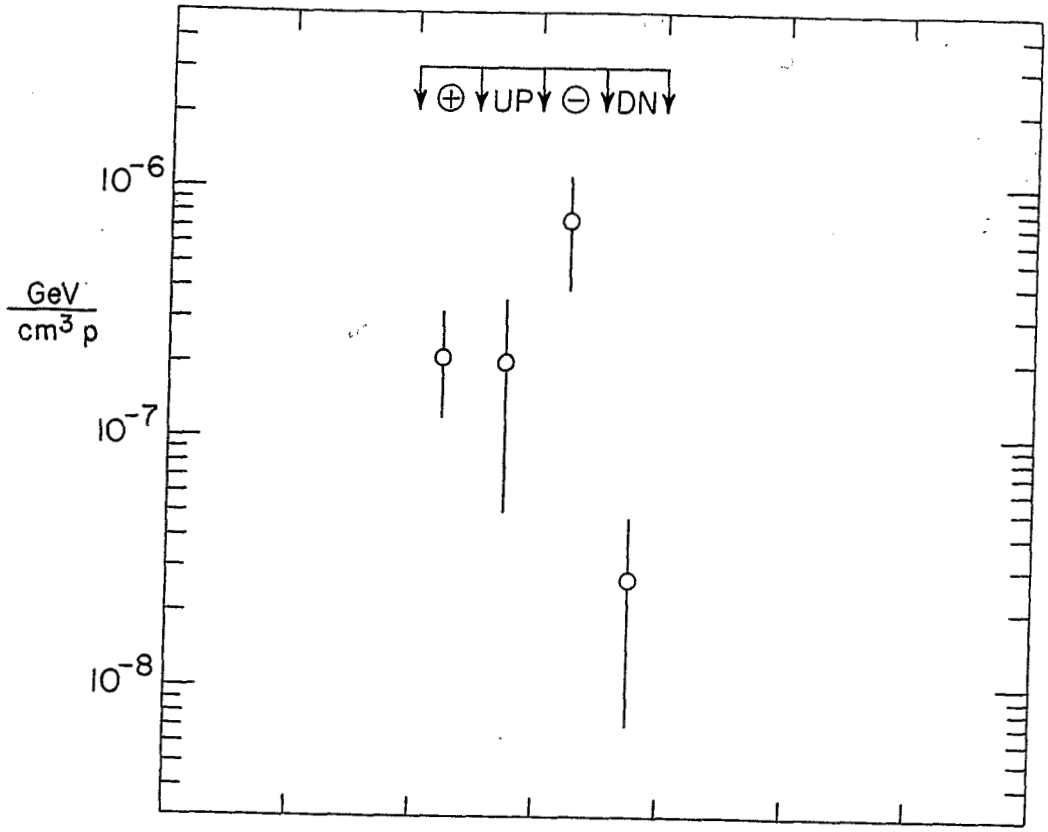

Fig. 7. Azimuthal dependence within last Z bin of B2I in Fig. 6. The symbol ⊕ designates the magnet quarter facing ring center. Forward neutrals would populate the opposite side, designated by ⊖.

dipoles.[13] Fig. 8 shows energy per incident within the magnet aperture at the exit of the indicated elements. The flat distribution beyond B1I is likely due to fast forward protons; these particles are still within the aperture for the magnets considered in this calculation.

We turn now to consideration of protons incident at larger depths from the edge of the dump. CASIM runs were made at 3 mm vertical displacement for the lattice elements described above, and at 1 cm displacement in a geometry where only Q3 was considered. At the 3 mm displacement, no energy within the aperture was observed beyond the exit of Q1 (see Fig. 8) for 240,000 incident primaries. The coil-averaged energy densities for all runs are shown in Fig. 9. The energy deposition density clearly falls rapidly with increasing displacement on the dump edge. This fall-off for Q3, the magnet with highest energy deposition density, is shown in Fig. 10, together with a curve which is the sum of two exponentials and which will be assumed to represent the functional dependence of energy deposition density on dump-edge displacement.

Conservatively allowing a factor of 4 for Z and φ variations within Q3, we obtain the following upper limit for energy deposition density as a function of distance from the dump edge, Y:

$$D(Y)[\mathrm{GeV/cc \cdot p}] = 2.4 \times 10^{-5} \cdot \mathrm{EXP}(-Y/.767) + 3.6 \times 10^{-7} \cdot \mathrm{EXP}(-Y/5.374)$$

with Y in mm.

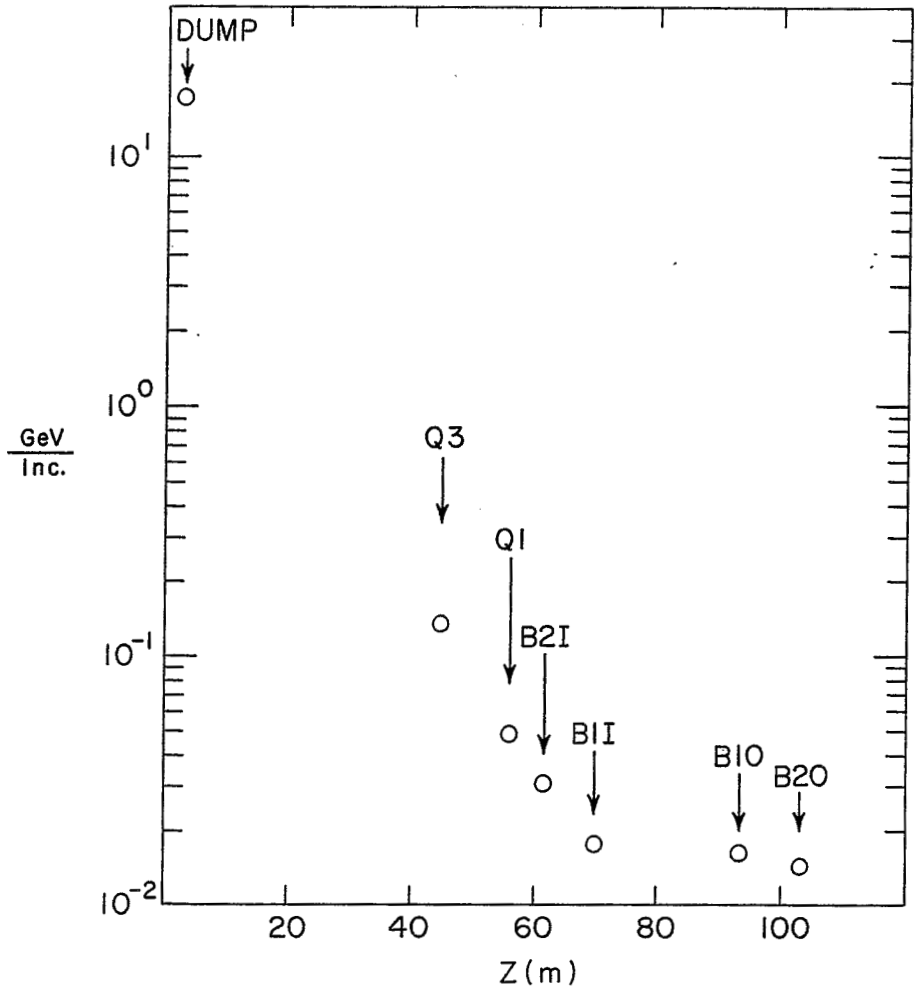

Fig. 8. Energy per incident within magnet aperture at exit of indicated element. Incident 250 GeV/c protons at 1 mm from edge of dump.

The current kicker is designed[1] to achieve an approximately uniform vertical displacement between 1.0 and 1.5 cm from the edge of the dump. Assuming, therefore, a uniform proton density of 2.28×10^{12} protons/mm, the maximum deposition density is calculated by multiplying this number times the expression above and integrating between 10 and 15 mm. The result is

$$D(MAX) = 4.15 \times 10^5 \text{ GeV/cc}$$
$$= 1.1 \times 10^{-2} \text{ mJ/g}$$

Since FNAL has established a quench limit of ~1 mJ/g,[14] loss from the internal dump would appear to be "safe" by 2 orders of magnitude.

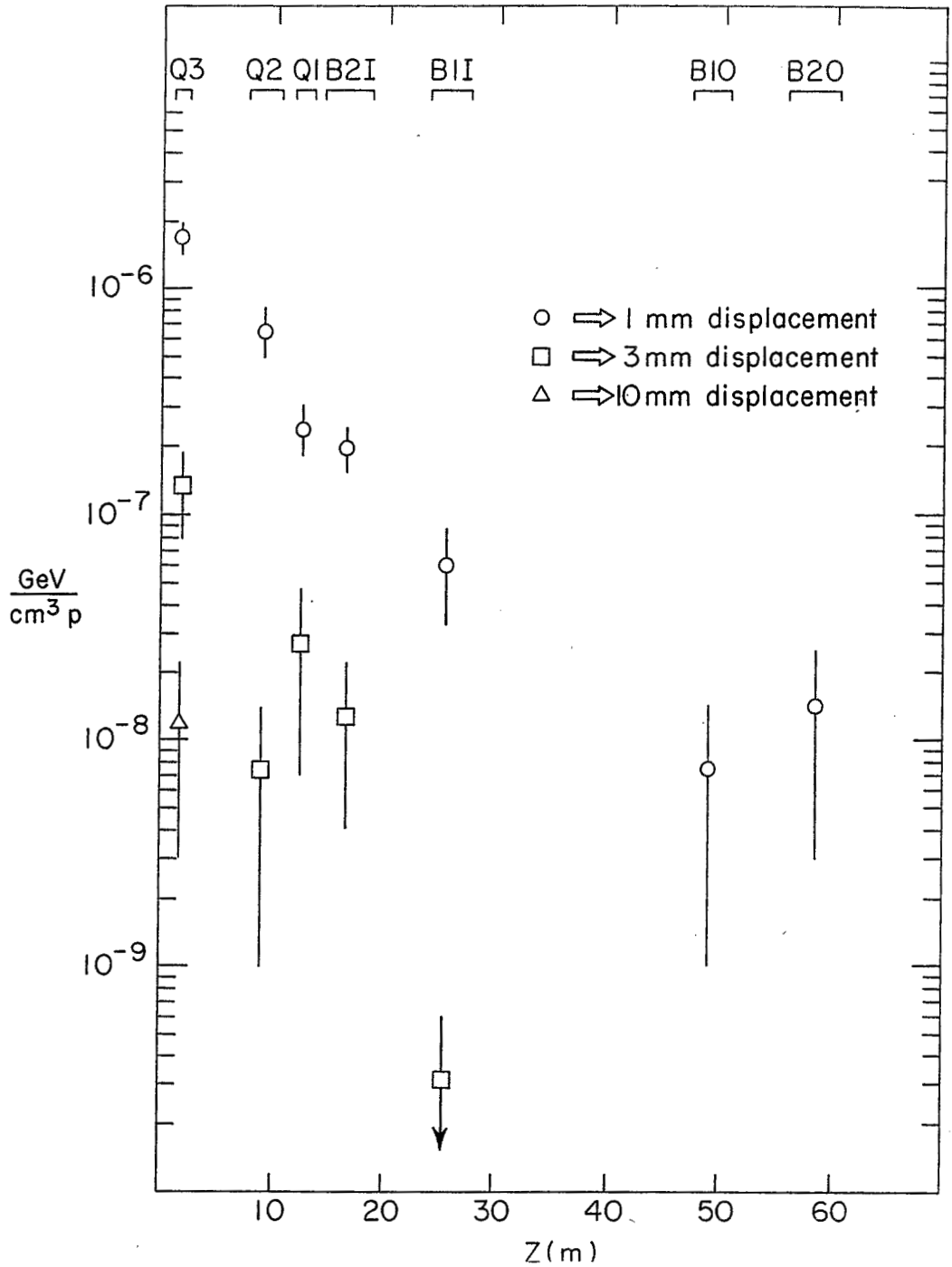

Fig. 9. Coil averaged energy densities. See Fig. 5 and text.

IV. Summary/Conclusions

An internal dump consisting of a titanium alloy window/beam pipe followed by graphite and steel regions would appear to be feasible as regards both dump survival and downstream magnet quenching. Survival depends critically on dispersing the beam on the face of the dump with a sweeping magnet; failure of the sweeping magnet would destroy the dump window for beam intensities considerably below the design value. Survival of the window also limits the intensity within a single bunch to values at or very near those of the

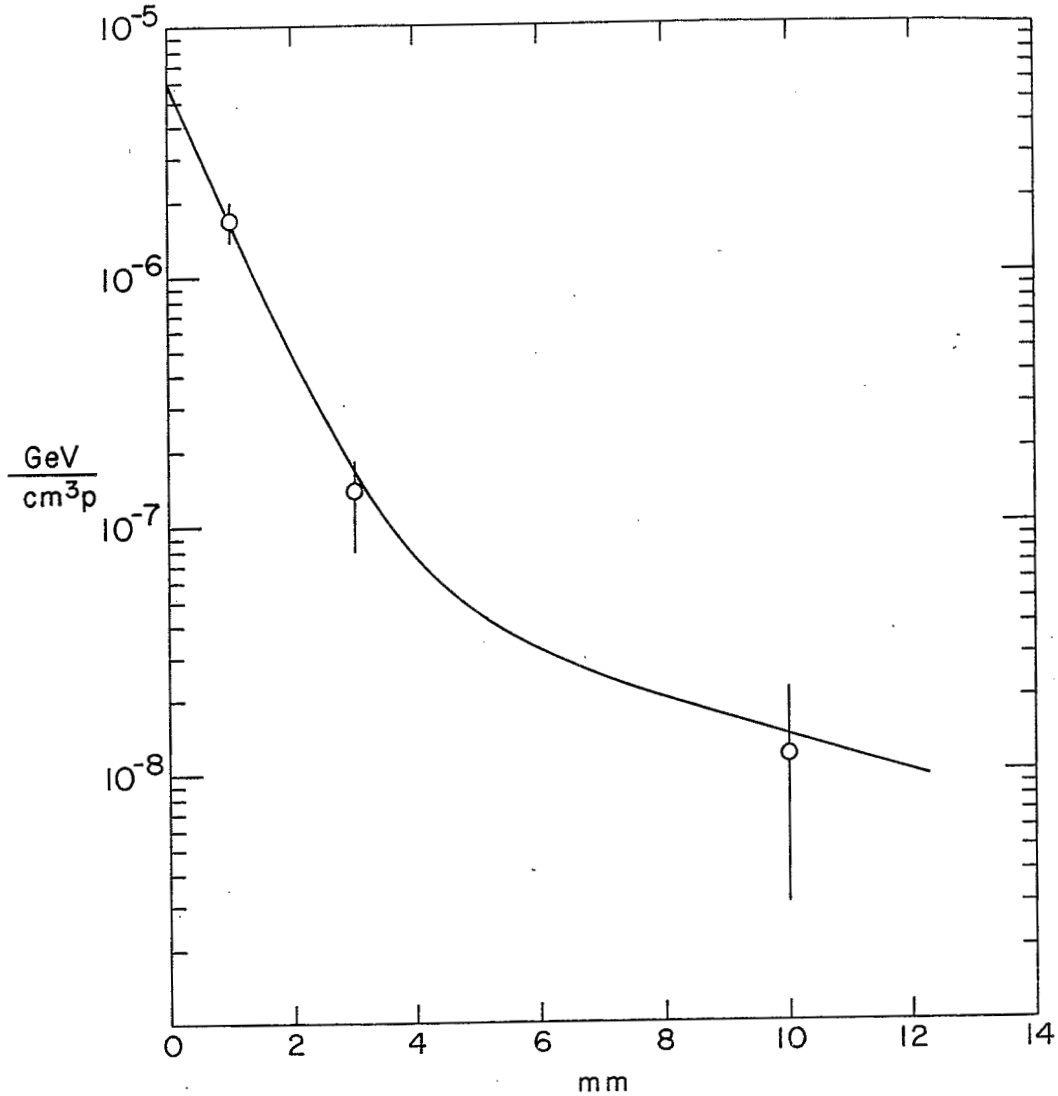

Fig. 10. Energy density in coil of Q3 as function of vertical displacement of incident beam from dump edge.

current design. Radiation heating of downstream magnets by energy escaping the dump is strongly dependent on the displacement from the dump edge achieved by the ejection kicker. A fast kicker synchronized to a gap in the circulating beam is expected to obtain a beam profile on the dump face which provides a two orders-of-magnitude safety margin against quenching downstream magnets.

The question of dump cooling, which may necessitate a closed water system within the dump if repetitive beam dumping is required, has not been addressed in this note and remains a topic for further study.

Footnotes/References

1. H. Foelsche, private communication. (A technical note describing dump location options, as well as dump kicker and sweeper specifications, is in preparation.)
2. Properties from "Materials Engineering," Vol. 82, No. 4, 1975. Courtesy of E.S. Rodger.
3. Conceptual Design of the Relativistic Heavy Ion Collider, BNL S1932, May, 1986.
4. J. Claus, private communication. The lattice parameters for this location are β_x=11.8310 m and β_y=28.1158 m for an insertion with a symmetric β of 6.0 m at the crossing point.
5. P. Sievers, "Elastic Stress Waves in Matter Due to Rapid Heating by an Intense High-Energy Particle Beam, CERN LAB II/BT 174-2, 1974. Although the dynamic stresses calculated here can be large, the amplification is due to high symmetry, which focuses reflected waves back to the origin of a circular disk. The RHIC situation is highly asymmetric.
6. We take twice the number of bunches given in the 1986 Conceptual Design. At the time of this writing, this "upgrade' is considered feasible.
7. A. Van Ginnekin, "CASIM. Program to Simulate Hadronic Cascades in Bulk Matter," Fermilab FN-272, 1975.
8. A. Stevens, "Improvement in CASIM; Comparison with Data," AGS/AD/Tech. Note No. 296, 1988.
9. A. Van Ginnekin, "Elastic Scattering in Thick Targets and Edge Scattering," Fermilab-Pub-87/141, 1987. This reference discusses problems associated with simulation of small energy loss processes. Interpolating results given in this reference for Al and Fe and using 1/P scaling indicate that ~78% of protons parallel to the beam direction at a transverse distance of 0.01 mm would scatter into the aperture.
10. Comparison with an unbiased version of CASIM was made for the first downstream magnet (Q3) and the results were in excellent agreement.
11. The B1 magnets are large aperture magnets shared by both beams. No attempt was made to accurately describe the geometry of these magnets.
12. The coil was approximated as iron at reduced (6.0 g/cc) density extending 1 cm in the radial (r) dimension. For binning purposes, the coils were typically divided into 4 to 5 regions in Z, 2 or 3 regions in r and 16 regions in azimuth.
13. A.J. Stevens, "Energy Deposition Densities Downstream of Isabelle Ejection Septa," ISABELLE Tech. Note 165, 1980.
14. A. Van Ginnekin, D. Edwards, and M. Harrison, "Quenching Induced by Beam Loss at the TEVATRON," Fermilab-Pub-87/113, 1987.